

## A Study of Wintertime Mixed-phase Clouds over Land Using Satellite and Aircraft Observations

Yoo-Jeong Noh<sup>1\*</sup>, J. Adam Kankiewicz<sup>2</sup>, Stanley Q. Kidder<sup>1</sup>, Thomas H. Vonder Haar<sup>1</sup>

<sup>1</sup> Cooperative Institute for Research in the Atmosphere (CIRA), Colorado State University, Fort Collins, CO 80523

<sup>2</sup> WindLogics Inc., 1021 Bandana Blvd. N., St. Paul, MN 55108

### 1. INTRODUCTION

Mixed-phase clouds consisting of both liquid and ice phase hydrometeors are relatively common in the real atmosphere (Deeter and Vivekanandan, 2004). Further understanding of mixed-phase clouds is essential for radar, lidar, satellite retrievals, climate/weather numerical modeling, and even aviation safety issues regarding icing conditions. Detection of mixed-phase clouds in which supercooled liquid water coexists with ice is an important and challenging problem and not fully understood yet. Moreover, mid-level mixed-phase clouds such as altocumulus and altostratus have not been paid attention as much as severe weather-related precipitating clouds in spite of covering over 22% of the earth's surface (Warren et al. 1986, 1988). Many remote sensing studies have treated mixed-phase clouds as to retrieve their physical properties are still limited than those for single-phase either ice or liquid clouds, even though they have different radiation characteristics than single phase clouds (Zhang and Vivekanandan 1999). Mixtures of liquid and ice in these clouds are often responsible for the uncertainties in radiative transfer modeling and satellite measurements.

Previous studies of mixed-phase clouds have been based on in-situ measurements since Cunningham (1951) such as Heymsfield et al. (1991), Field 1999, Cober et al. (2001), Lawson et al. (2001), Fleishauer et al. (2002), and Carey et al. (2007). For example, Cober et al. (1995) reported thin cloud-top layers of supercooled water at temperatures lower than  $-10^{\circ}\text{C}$  with ice virga below. Rauber and Tokay (1991) investigated a supercooled water layer at cloud top analyzing numerous observations. Fleishauer et al. (2002) and Niu et al. (2006) also observed a common structure consisting of a supercooled liquid layer on top and ice particles below from in-situ airborne observations focused on the mid-level, mixed-phase clouds during the Cloud Layer Experiments (CLEXs). Shupe et al. (2004) used Doppler spectrum observations from ground-based 35 and 94 GHz Doppler radars to identify and quantify the microphysical properties of both phases in a mixed-phase cloud for during the summer seasons over Florida. In spite of various positive results, they also They found the

distinction between liquid droplets and small ice crystals in mixed-phase clouds is challenging, at best, using only millimeter Doppler radars.

Wang et al. (2004) developed a retrieval algorithm of altocumulus with ice virga that they separately treated as a cirrus-like part and a supercooled liquid part using ground measurements such as lidar, radar, microwave radiometer, and IR spectrometer. Deeter and Vivekanandan (2004) presented a case study of mixed-phase clouds over land using AMSU-B (Advanced Microwave Sounding Unit-B) and ground-based remote sensing observations of a system of mixed-phase non-precipitating clouds. Their results indicate that the application to mixed-phase clouds, of millimeter-wave-based retrieval algorithms developed specifically for single-phase clouds, is generally not appropriate.

In general, studies of cloud phase-composition for mixed-phase clouds have been significantly limited by a lack of intensive in-situ measurements that can directly explicitly discriminate between the ice and liquid phases. Our limited knowledge of mixed-phase cloud structure and characteristics has caused these clouds to be poorly represented in weather/climate models and satellite retrievals. Gayet et al. (2002) indicated that satellite-based retrievals of mixed-phase cloud structure may be severely compromised because the scattering properties near cloud top were mostly dominated by water droplets.

In this study, three mid-level, mixed-phase cloud cases observed over Ontario, Canada during the C3VP/CLEX-10 field experiment are analyzed. We will try to interpret and characterize the vertical structure of mixed-phase clouds as detected by various remote sensors. Through the study, we attempt to answer the following questions: What are the important features of mixed-phase clouds detected by various remote sensors from aircraft and satellite observations? How are liquid/ice phase hydrometeors vertically distributed in the clouds? How do mixed-phase clouds respond to microwave frequencies currently available? Preliminary results from in-situ aircraft and satellite measurements are presented.

### 2. DATA

In this study, aircraft observations during C3VP/CLEX10 are shown. The CLEX (Fleishauer et al. 2002; Niu et al. 2006; Carey et al. 2007) is part of an ongoing effort funded by the Department of Defense's Center for Geosciences/Atmospheric Research to observe and characterize the microphysical properties,

---

\* Corresponding author address: Yoo-Jeong Noh, Cooperative Institute for Research in the Atmosphere/ Colorado State University, Fort Collins, CO 80523; Noh@cira.colostate.edu

dynamics and morphology of non-precipitating, mid-level, mixed-phase clouds started in 1996 (see [http://www1.cira.colostate.edu/GeoSci/CLEX/clex\\_main/clex10/clex10.html](http://www1.cira.colostate.edu/GeoSci/CLEX/clex_main/clex10/clex10.html)). The C3VP is the extensive validation of the satellite products performed by the Meteorological Service of Canada as part of the international CloudSat program (see <http://c3vp.org>) with the primary objective to validate measurements and retrieved products from the CloudSat and CALIPSO satellites. These two field experiments worked together during 2006-2007 winter seasons to target A-Train (the Afternoon satellite constellation led by NASA's Aqua satellite) overpasses of winter season clouds and precipitation over the southern Ontario region of Canada.

Additionally, various kinds of satellite data are also used to investigate responses of these mid-level mixed-phase clouds in satellite microwave channels. The AMSU-B onboard NOAA satellite series has two high-frequency window channels at 89 and 150 GHz, and three water vapor channels at  $183.3 \pm 1$ ,  $183.3 \pm 3$ , and  $183.3 \pm 7$  GHz (Zhao and Weng, 2002). The AMSU-B crossly scans  $\pm 47^\circ$  from nadir, covering approximately a 2000 km wide swath. The spatial resolution at nadir is  $\sim 15$  km. The AMSR-E (Advanced Microwave Scanning Radiometer-EOS) is one of the six sensors aboard the Aqua satellite. This passive microwave radiometer has vertically and horizontally polarized 6.6, 10.7, 18.7, 21, 36.5, and 89 GHz channels and vertically polarized 50 and 53 GHz channels. It conically scans the Earth with an incident angle of about  $55^\circ$  to the normal of the Earth's surface. The swath width is about 1600 km. Spatial resolutions of the pixels at 36.5 and 89 GHz examined in this study are about  $8 \times 14$  km<sup>2</sup> and  $4 \times 6$  km<sup>2</sup>, respectively. MODIS (Moderate-Resolution Imaging Spectroradiometer) images (12  $\mu$ m) of the Aqua satellite are used to examine cloudy areas of interest (not shown here). For studying the vertical structure of clouds, data from the recently launched CloudSat (Stephens et al. 2002) are used together with coincidental aircraft observations. CloudSat is designed to measure the vertical structure of clouds and precipitation from space with a 94-GHz cloud profiling radar (CPR), which observes most of the cloud condensate and precipitation within its nadir field of view and provides profiles of these properties with a vertical resolution of 500m. CloudSat release-version 04 data are used in this study (refer to <http://cloudsat.cira.colostate.edu/> for more details).

### 3. AIRBORNE AND SATELLITE OBSERVATIONS

During C3VP/CLEX10 the microphysical structure of several mixed phase clouds were sampled using in-situ probes and remote sensing instruments onboard the National Research Council of Canada's Convair-580 aircraft. Preliminary results of three cases (31 October 2006, 5 November 2006, and 25 February 2007) are presented here.

The first flight during C3VP/CLEX10 occurred on 31 October 2006. An approaching cold front triggered extensive cloudiness over Southern Ontario. Figure 1

shows vertical profiles of temperature/dew point and liquid/ ice water content (LWC and IWC) obtained from Convair-580 aircraft observation at 182230-184225 UTC. The full flight track is also shown in Fig. 1c where the plotted leg is colored with red. It is noted that LWC and IWC are from the King liquid water and Nevzorov LWC-TWC probes, which have cleared the first data quality control check. The cloud observed here consisted of two layers, with an upper-layer cloud top temperature of  $-21^\circ\text{C}$ . As shown in Fig. 1a, both layers of this cloud are dominated by supercooled liquid droplets. In this case, IWC is very small, not exceeding  $0.01 \text{ gm}^{-3}$ .

On 5 November 2006, a warm front had moved over Southern Ontario leaving behind a large area of mid-level cloud cover. Mid-level clouds were observed at a C3VP ground station continuously for over ten hours. During the flight targeting the CloudSat overpass around 1830 UTC, a mixed phase cloud layer, with nearly 3 km of thin cirrus above and scattered clouds below, was observed. As shown in Fig. 2, although the target mixed-phase cloud has cloud top temperatures down to  $-22^\circ\text{C}$ , a significant amount of liquid up to  $0.3 \text{ gm}^{-3}$  is observed in the cloud (4-4.7 km), indicating this cloud also has the classic CLEX profile of liquid.

Finally, on 25 February 2007 a large low-pressure system over the central US continued to move slowly toward the northeast, near southern Ontario. Ahead of the system, a band of cirrus and a large area of mid-level cloud cover followed by precipitating nimbostratus were observed over our area. During the flight, layers of altostratus cloud were sampled. The selected flight leg plotted in Fig. 3 is a descending flight track. Similar to the other cases, the maximum of liquid water (about  $0.15 \text{ gm}^{-3}$ ) appears at the cloud top. The temperatures throughout the cloud (5.8-6.7 km) are all below  $-20^\circ\text{C}$ . In this case, IWC has the highest value of  $0.07 \text{ gm}^{-3}$  at the top, but a significant amount of ice also is found near the bottom part of the cloud ( $\sim 6$ km).

Figure 4 shows cloud classifications from the CloudSat product, 2B-CLDCLASS for the three cases. The current CloudSat algorithm classifies clouds into St, Sc, Cu, Ns, Ac, As, deep convective, or high cloud (Ci) by combining space-based active (CPR and CALIPSO lidar) and passive remote sensing (MODIS) data. The high cloud class consists of cirrus, cirrocumulus, and cirrostratus. On 31 October 2006, altostratus cloud is mainly observed with some cirrus and stratocumulus cloud present. Altocumulus and altostratus cloud is observed, respectively, on 5 November 2006 and 25 February 2007 over the C3VP/CLEX10 target areas. Results show that CloudSat cloud classification products are in quite good agreement with the aircraft data.

In comparisons with liquid and ice water contents from airborne observations (Figs.1-3), retrieved satellite measurements (CloudSat product, 2B-CWC-RO) are shown in Fig. 5. Given the homogeneous nature of the clouds sampled and the relative closeness between the CloudSat and aircraft measurements, we assume here that the same clouds were sampled by both. The 31 October 2006 case (Fig. 1b and Fig. 5a) shows two

maxima of LWC clearly found in both dataset with similar observed values ( $\sim 0.2$  and  $\sim 0.4 - \sim 0.6 \text{ gm}^{-3}$ ), but with LWC locations slightly lower in CloudSat data. For the second case, 05 November 2006 (Fig. 2b and Fig. 5b), the amount of CloudSat retrieved LWC is slightly less with a maximum around 4.5km. However, the bottom layer of cloud observed at 2 km in the CloudSat data was not sampled during the aircraft observations. Interestingly, the 25 February 2007 case (Fig. 3b and Fig. 5c) has both datasets have similar peak values of LWC but at different vertical locations. In Fig. 3b, the aircraft LWC and IWC measurements have maximum values of 0.12 and 0.07  $\text{gm}^{-3}$  around 6.5 km, while the CloudSat data shows large amounts of ice (up to 0.4  $\text{gm}^{-3}$ ) at the same height. From Fig. 5c, a CloudSat LWC maximum appears near the cloud bottom, but instead the second maximum of IWC is found below from aircraft measurements as shown in Fig. 3b. This result suggests that some of IWC at cloud top retrieved from CloudSat data could be possibly supercooled liquid water in spite of low temperatures. Also, it is noted for these three cases LWC from the aircraft measurements tend to increase with altitude in each single layer with 200-800 m depth as reported by Fleishauer et al. (2002), but CloudSat LWC shows bell-shaped patterns.

Next, in order to understand how liquid and ice hydrometeors respond at microwave frequencies, brightness temperatures in various satellite passive microwave channels and their combinations are analyzed, and with some preliminary results are presented here.

The Aqua satellite passed over this area at 1800 UTC on 25 February 2007. Although there are frequencies from 6.6 to 89 GHz in AMSR-E, only 36.5 and 89 GHz are examined in the study. Figure 7a shows the horizontal distributions of vertically and horizontally polarized brightness temperatures at 89 GHz (36.5 GHz observations are not shown here). Fine features can be identified from images of all the four variables, which are influenced by both clouds and land surfaces. Since emission from land surface is more complicated than ocean surface, it is harder to interpret the signals from satellite data. It is seen that there are several signals between 42-46°N along the CloudSat track (black solid lines), especially around the Lake Ontario in Fig. 6a. In general lower brightness temperatures are observed over land than those found over water surfaces due to their different surface emissivities, although there are some scattering signatures, as indicated by large brightness temperatures, decreases are still clearly detected at 89 GHz over all surface types in the domain. The wide variations in brightness temperatures observed over the lakes also suggest there are frozen parts of the lakes (Huron, Ontario, and Erie). To further elaborate, cross sections of the brightness temperatures along the CloudSat track are shown in Fig. 6b. Over the C3VP/CLEX10 target region (pink circle and arrow bars), the area of 44-44.3°N that is part of a large cloud system covering the Lake Ontario region shows larger decreases in both polarized brightness temperatures at 89 GHz and the difference of vertically polarized brightness temperatures between 89 and 36.5 GHz

(about -20 K), compared with other surrounding areas in Fig. 6b except for the lake areas (cyan-shaded). The signals appear to be contaminated by surface effects, but could possibly contain evidence of ice phase in clouds that can be found by examining various combinations of brightness temperatures at different frequencies such as the difference between 89 and 36.5 GHz.

Figure 7 shows AMSU-B brightness temperatures at four channels of 89, 150, 183±1, and 183±7 GHz (the 183±3 GHz image, not shown here, appears to be between those of 183±1 and 183±7 GHz) on 31 October 2006. The NOAA-17 satellite passed over the area around 1700 UTC before the passage of A-Train satellites. Note that the microwave window channels (89 and 150 GHz) are sensitive to surface temperature and emissivity, but the water vapor channels are more sensitive to the atmospheric temperature and water vapor profiles (Deeter and Vivekanandan 2004). Also, brightness temperatures for all of the water vapor channels tend to decrease with increasing liquid water (ice), while increasing liquid tends to increase (decrease) the brightness temperature in the window channels (Cordisco et al. 2006). For this case, since the 89 and 150 GHz brightness temperatures seem to be affected by the cold surface temperatures, we use brightness temperature depressions ( $= T_B - T_{B,bg}$ ), where  $T_{B,bg}$  (background brightness temperature) is obtained by a histogram analysis of AMSU-B brightness temperature ( $T_B$ ) data from October 2006 to February 2007 at each frequency over each surface type. Though surface contamination is still an issue, its effects are greatly dampened by this method.

In this case, broad cloudy areas including the C3VP/CLEX10 target region (red circle) are seen in Fig. 7a. Due to the coarser spatial resolution of AMSU-B, the images appear lack of fine structures compared with those from AMSR-E as shown in Fig. 6. Nevertheless, low brightness temperature cells embedded on a large cloudy area are well found in Fig. 7. Any significant depression over the C3VP/CLEX10 region (red circle) is not found in the cross-section plots but relatively large depressions in all channels are shown over another cloudy area colored with pink, even though the values greatly vary at each frequency. They may be induced by ice particles in clouds.

Among AMSU-B channels, water vapor channels (183GHzs) are less sensitive to the surface conditions. Overall, 183±7 and 150 GHz are slightly more sensitive to the clouds with respect to the scattering. Both signals from liquid and ice phases of the mid-level mixed-phase clouds appear relatively weak and so complicated in the satellite microwave data. Moreover, it is not easy to interpret the signatures from the clouds over complex surfaces. Since surface temperatures and emissivities are highly variable in this region, particularly during winter seasons, we should carefully consider them. The results also show that measurements in various channels and their combinations should be considered to more accurately understand how liquid and ice hydrometeors respond to microwave frequencies.

#### 4. SUMMARY

In this study, preliminary results of measurements taken in wintertime mid-level mixed-phase clouds are presented. Satellite passive/active microwave observations and aircraft in situ measurements during the C3VP/CLEX10 field experiment are used to understand the characteristics of the mixed-phase clouds from various remote sensors and their microphysical features.

From the analysis of CloudSat standard data products and C3VP/CLEX10 measurements, first it is found that the amount of cloud water content (LWC and IWC) varies significantly in each case. However, no significant correlation is found between LWC and IWC. Also, any correlation between water content and temperature is not found. It is noted for three cases chosen in this study that a significant amount of liquid water is obtained from the aircraft observation in very low temperature conditions ( $< -20^{\circ}\text{C}$ ) at or near cloud top, reconfirming previously observed results (e.g., Fleishauer et al., 2002). Particularly interesting were LWC values up to  $0.3\text{ g/m}^3$  observed near cloud top between 4 and 4.7 km at temperatures near  $-22^{\circ}\text{C}$  on 5 November 2006.

Analyses of these clouds using satellite passive microwave data such as AMSR-E and AMSU-B are also ongoing. They give so far only limited information from mixed-phase clouds over land due to the land surface effects. Overall, the small features of mixed-phase clouds are not clearly discernable. Signals from liquid and ice phases of these mixed-phase clouds in the satellite passive microwave frequency measurements are relatively weak and so complicated compared with deep convective precipitating clouds (e.g., Noh et al., 2006) because mixed-phase clouds are relatively thin and temporally unstable. Also, for these clouds over land with complex surface conditions, land surface effects make it more difficult to interpret passive microwave satellite data. However, methods to detect mixed-phase clouds over land – such as background brightness temperature removal or brightness temperature combinations at different frequencies – do show future promise.

From the results, we confirm that the detection and characterization of mixed-phase clouds needs multi-frequency and multi-instrument analyses (e.g., CloudSat + CALIPSO + MODIS). It is also noted that more intensive observations are necessary to improve our understanding of mixed-phase clouds and their radiative properties. CloudSat makes it possible, for the first time, to have vertical profile information of cloud hydrometeors from around the globe in detail. CloudSat products are being validated and improved by using intensive in-situ observations taken during C3VP/CLEX10. As more datasets from the C3VP/CLEX10 field experiment become available in near future, further detailed studies will continue using various airborne and satellite measurements.

#### 5. ACKNOWLEDGMENTS

This research was supported by the Department of Defense Center for Geosciences/Atmospheric Research at Colorado State University under Cooperative Agreement W911NF-06-2-0015 with the Army Research Laboratory.

#### REFERENCES

- Carey, L. D., J. Niu, P. Yang, J. A. Kankiewicz, V. E. Larson, and T. H. Vonder Haar, 2007: The vertical profile of liquid and ice water content in mid-latitude mixed-phase altocumulus clouds. *J. Appl. Meteor. Climatol.*, accepted.
- Cober, S. G., G. A. Isaac, A. V. Korolev, and J. W. Strapp, 2001: Assessing cloud-phase condition. *J. Appl. Meteor.*, **40**, 1967-1983.
- Cordisco, E., C. Prigent, and F. Aires, 2006: Snow characterization at a global scale with passive microwave satellite observations. *J. Geophys. Res.*, **111**, D19102, doi:10.1029/2005JD006773.
- Cunningham, R. M., 1951: Some observations of natural precipitation processes. *Bull. Amer. Meteor. Soc.*, **32**, 334-336.
- Deeter, M. N. and J. Vivekanandan, 2004: AMSU-B observations of mixed-phase clouds over land. *J. Appl. Meteor.*, **44**, 72-85.
- Field, P. R., 1999: Aircraft observations of ice crystal evolution in altostratus cloud. *J. Atmos. Sci.*, **56**, 1925-1941.
- Fleishauer, R. P., V. E. Larson, and T. H. Vonder Haar, 2002: Observed Microphysical structure of mid-level, mixed-phase Clouds. *J. Atmos. Sci.*, **59**, 1779-1804.
- Gayet, J.-F., S. Asano, A. Yamazaki, A. Uchiyama, A. Sinyuk, O. Jourdan, and F. Auriol, 2002: Two case studies of winter continental-type water and mixed-phase stratocumuli over the sea. 1. Microphysical and optical properties. *J. Geophys. Res.*, **107**, D21, 4569, doi:10.1029/2001JD001106.
- Heymsfield, A. L., L. M. Milosevich, A. Slingo, K. Sassen, and D. O'C. Starr, 1991: An observational and theoretical study of highly supercooled altocumulus. *J. Atmos. Sci.*, **48**, 923-945.
- Korolev, A. V., G. A. Isaac, S. G. Cober, J. W. Strapp, and J. Hallett, 2003: Microphysical characterization of mixed-phase clouds. *Q. J. R. Meteor. Soc.*, **129**, 39-65.
- Lawson, R. P., B. A. Baker, C. G. Schmitt, and T. L. Jensen, 2001: An overview of microphysical properties of arctic clouds observed in May and July during FIRE ACE. *J. Geophys. Res.*, **106**, 14989-15014.
- Niu, J., L. D. Carey, P. Yang, J. A. Kankiewicz, and T. H. Vonder Haar, 2006: A common microphysical structure for mid-level mixed phase clouds in the mid-latitudes: Results from the Cloud Layer Experiment (CLEX-9). American Meteorological Society, *12th Conference on Cloud Physics*, Paper P1.25, July 2006.

- Noh, Y. J., G. Liu, E. K. Seo, J. R. Wang, and K. Aonashi, 2006: Development of A Snowfall Retrieval Algorithm at High Microwave Frequencies. *J. Geophys. Res.* **111**, D22216, doi:10.1029/2005JD006826.
- Rauber, R. M., and A. Tokay, 1991: An explanation for the existence of supercooled water at the tops of cold clouds. *J. Atmos. Sci.*, **48**, 1005-1023.
- Shupe, M. D., P. Kollias, S. Y. Matrosov, and T. L. Schneider, 2004: Deriving mixed-phase cloud properties from Doppler radar spectra, *J. Atmos. Ocean. Tech.*, **21**, 660-670.
- Stephens, G. K., et al., 2002: The CLOUDSAT Mission and the A-Train – A new dimension of space-based observations of clouds and precipitation, *Bull. Amer. Meteor. Soc.*, **83**, 1771-1790.
- Wang, Z., K. Sassen, D. N. Whiteman, and B. B. Demoz, 2004: Studying Altocumulus with ice virga using ground-based active and passive remote sensors. *J. Appl. Meteor.*, **43**, 449-460.
- Warren, S. G., J. Hahn, J. London, R. M. Chervin, and R. Jenne, 1988a: Global distribution of total cloud cover and cloud type amount over land. NCAR Tech. Note TN-317 STR, 212 pp.
- Warren, S. G., J. Hahn, J. London, R. M. Chervin, and R. Jenne, 1986: Global distribution of total cloud cover and cloud type amount over land. NCAR Tech. Note TN-273+STR, 29 pp.+200 maps.
- Warren, S. G., J. Hahn, J. London, R. M. Chervin, and R. Jenne, 1988: Global distribution of total cloud cover and cloud type amount over ocean. NCAR Tech. Note TN-317+STR, 41 pp.+170 maps.
- Zhang G., and J. Vivekanandan, 1999: Microwave radiation from mixed phase cloud and parameter retrievals, Geoscience and Remote Sensing Symposium, 1999. IGARSS '99 Proceedings. IEEE 1999 International, **4**, 2182-2184, 28 June – 02 July 1999, Hamburg, Germany.
- Zhao, L., and F. Weng, 2002: Retrieval of ice cloud parameters using the Advanced Microwave Sounding Unit. *J. Appl. Meteor.*, **41**, 384–395.

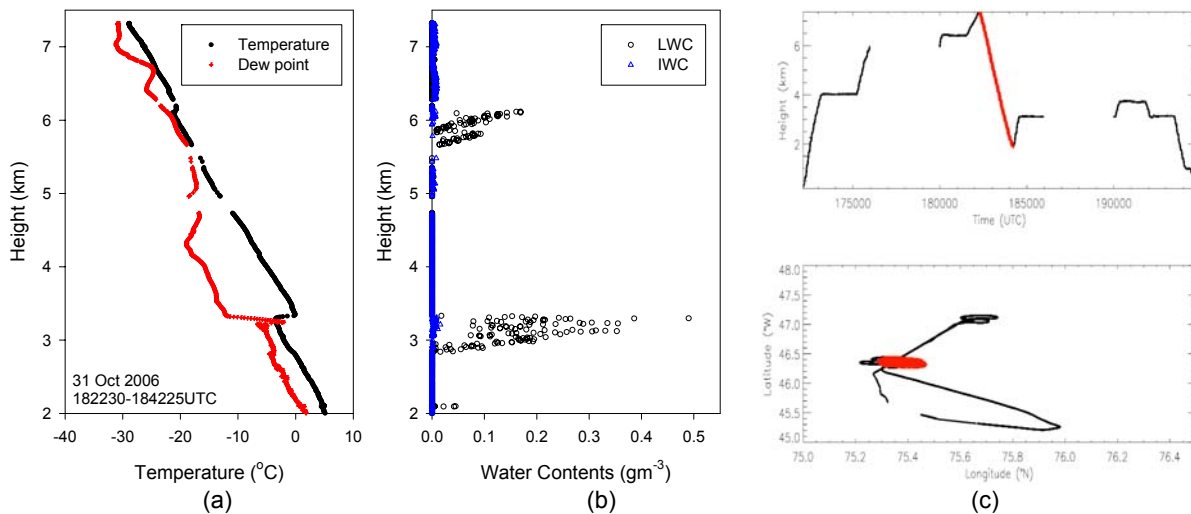


Figure 1. Vertical profiles of (a) temperature and dew point and (b) liquid (LWC) and ice (IWC) water contents obtained from the aircraft observation on 31 October 2006 (182230-184225 UTC) during C3VP/CLEX10. The selected leg is colored red in the full flight track (c).

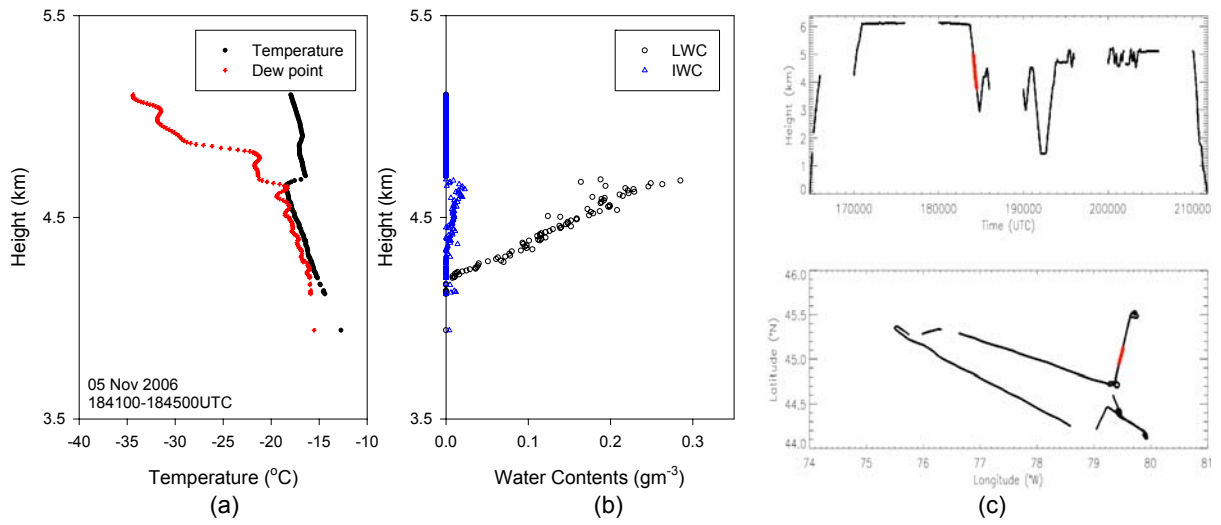


Figure 2. Same as Fig. 1 but for 05 November 2006 (184100-184500 UTC).

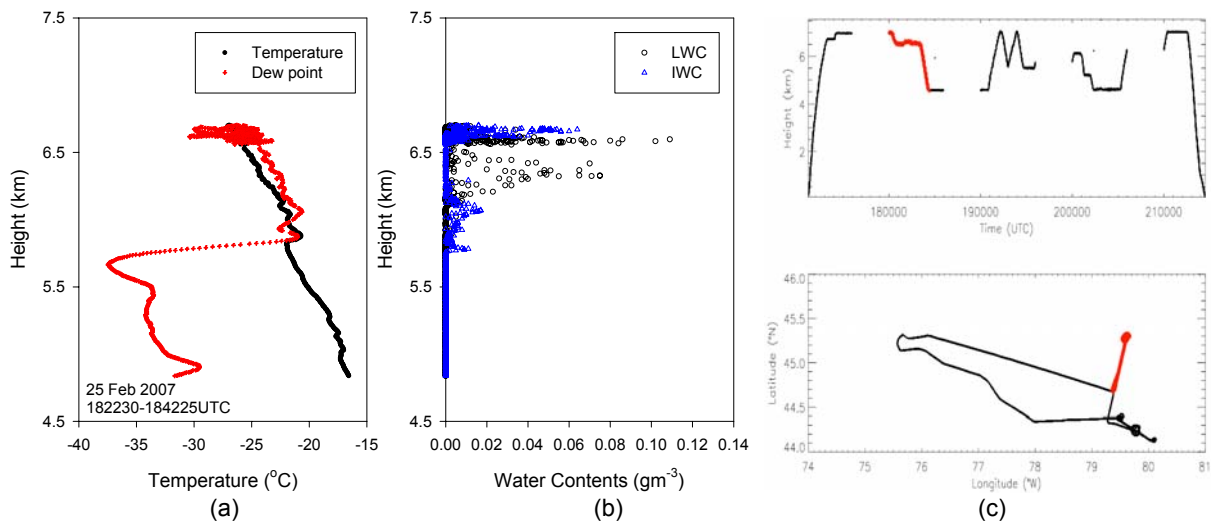


Figure 3. Same as Fig. 1 but for 25 February 2007 (182230-184225 UTC).

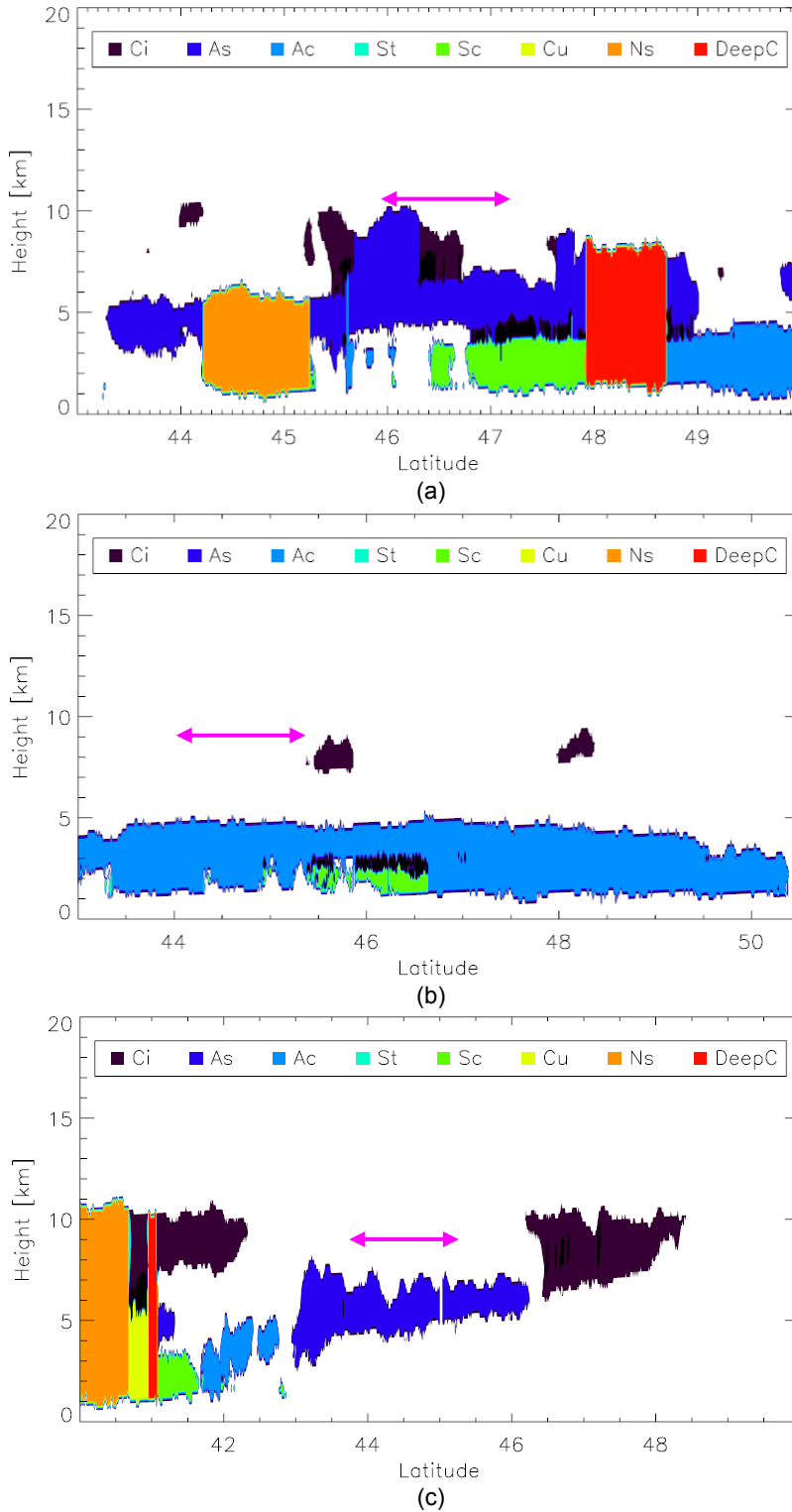


Figure 4. CloudSat cloud classifications for (a) 31 October 2006, (b) 5 November 2006, and (c) 25 February 2007. C3VP/CLEX10 target regions are represented as pink arrow bars.

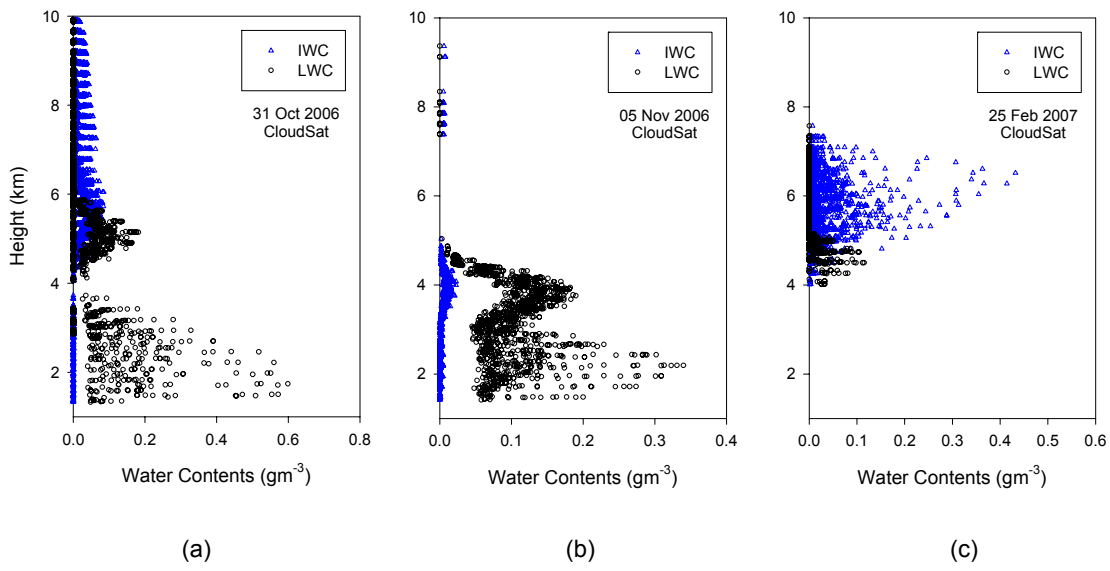
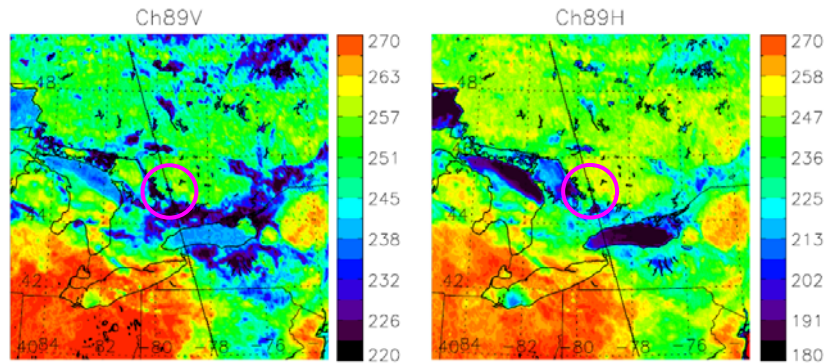
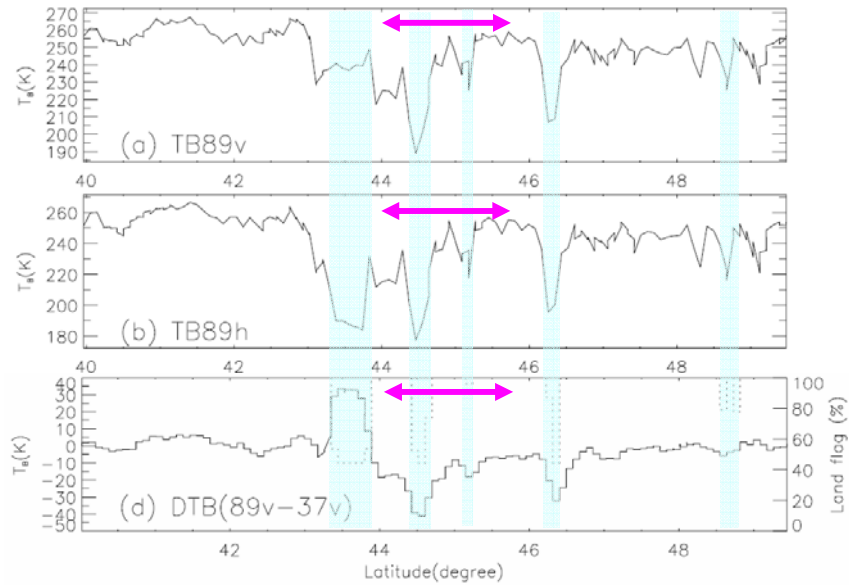


Figure 5. Vertical profiles of liquid (LWC) and ice (IWC) water contents from CloudSat (2B-CWC-RO, Ver.04) over each C3VP/CLEX10 target region for (a) 31 October 2006, (b) 05 November 2006, and (c) 23 February 2007 cases.

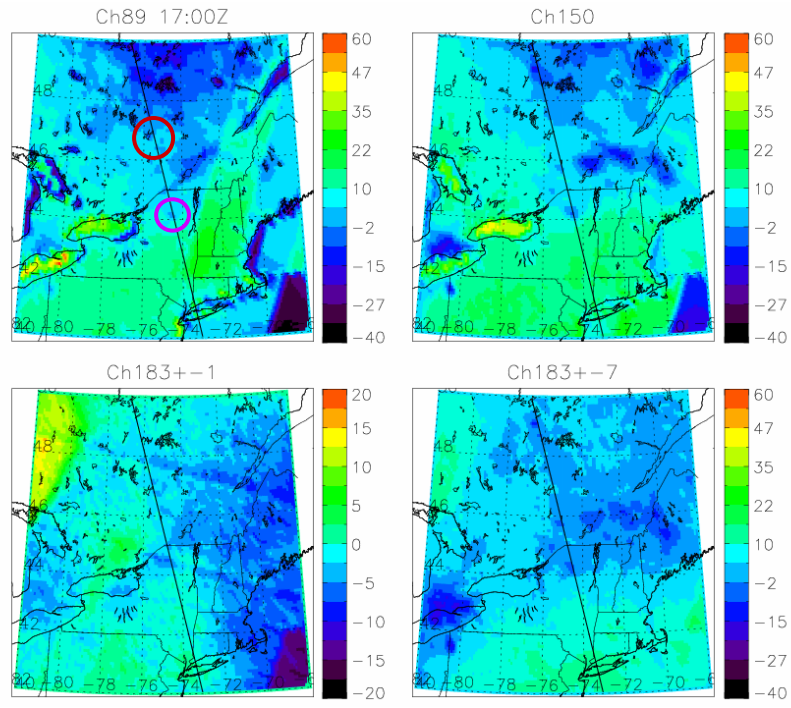


(a)

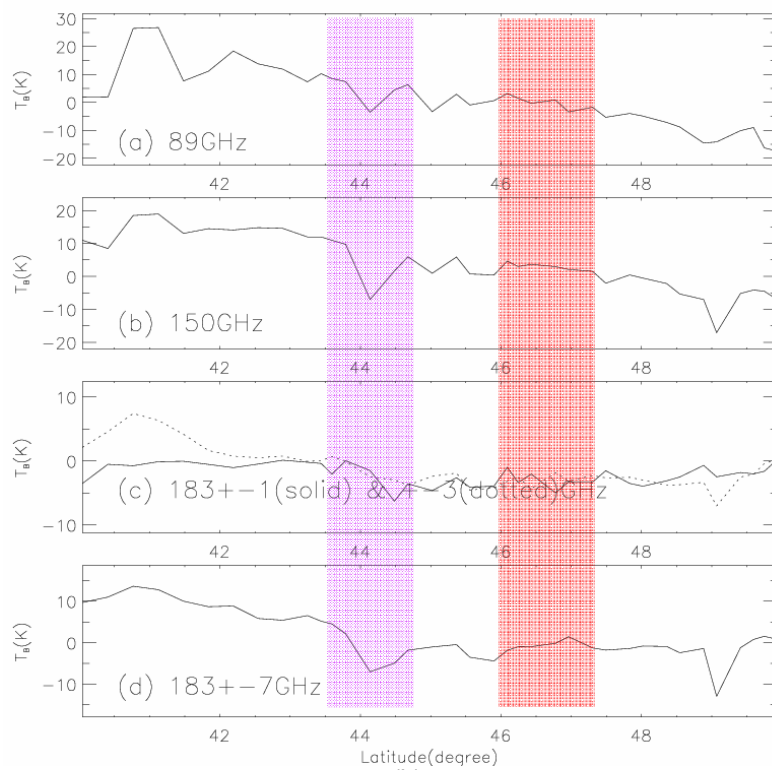


(b)

Figure 6. AMSR-E horizontally and vertically polarized brightness temperatures at 89 GHz (a) and their cross-sections including the difference between 89 GHz and 36.5 GHz (b) along the CloudSat overpass track shown as black lines in (a) on 25 February 2007. The pink circles and arrow bars indicate the C3VP/CLEX10 target area. Lake areas are cyan-shaded in (b).



(a)



(b)

Figure 7. AMSU-B brightness temperature depressions at 89-, 150-, and two 183-GHz frequencies with the CloudSat overpass track (black solid line) (a) and the cross-sections (b) on 31 October 2006. The red (C3VP/CLEX10 target region) and pink circled areas of (a) are respectively shaded with red and pink in (b).